Proceedings of the 11th ICPMG 2026
11th International Conference on Physical Modelling in Geotechnics
8-12 June 2026, Zurich, Switzerland

Small-scale physical modelling of trees subject to cyclic and monotonic loading

J.A. Knappett
University of Oxford, Oxford, UK, jonathan.knappett@eng.ox.ac.uk

G.S. Georgiev
WSP, UK, gxgeorgiev93@gmail.com

X. Zhang
Nanjing University of Aeronautics and Astronautics, PR China, x.y.zhang@nuaa.edu.cn

M.O. Ciantia
University of Dundee, Dundee, UK, m.o.ciantia@dundee.ac.uk

ABSTRACT: The push-over behaviour of trees under extreme loading associated with natural hazards is important in Forestry and Civil Engineering. Strong winds can damage stands of commercial timber and blow down trees which block transport infrastructure or damage overhead power and telecommunication lines. Debris flows may also load trees located on steep slopes next to transport infrastructure. This paper will present results from a preliminary 1-g physical modelling study of 3D-printed tree root systems subjected to cyclic and/or monotonic load histories. Appropriate scaling laws are first established to account for stress-level on soil dilatancy and peak strength through comparison of 1-g and centrifuge test data. Subsequently, behaviour under one-way cyclic loading representative of wind loading (pre-conditioning/shake-down), followed by monotonic push-over (representative of extreme events). The direction of these loads relative to each other is varied to consider different idealised field scenarios. The results indicate that prior cyclic loading can influence moment capacity depending on the relative directionality of cyclic to monotonic loading. Directionality is less significant for rotational stiffness evolution, which appears to universally increase with continued cyclic loading tend. These findings have implications for physical and numerical modelling of tree pushover, risk assessment and for field evaluation of tree characteristics.

1 INTRODUCTION

The pushover response of trees to lateral loads is important for several applications in Civil Engineering and Forestry. From an engineering perspective, trees situated close to buildings or other infrastructure (e.g. highways, railway overhead power lines) can pose a hazard in high winds, resulting in damage, disruption to transport systems and even fatalities (e.g. Schmidlin 2009). In Forestry, commercial timber stands can be damaged due to high winds (‘windthrow’), resulting in economic losses (McCarthy et al. 2010). Overturning of trees located on slopes can even be a trigger for landsliding (Jakob and Lambert 2009).

In principle, the moment capacity of trees can be quantified using a range of methods, including empirical approaches (e.g. Achim and Nicoll 2009) and methods that treat the root system of the tree as an equivalent shallow foundation (e.g. Dattola et al. 2020; Zhang et al. 2023). However, these methods suffer from difficulty in field conditions not always matching those used in empirical databases and in quantifying the depth and spread of the root system.

As a result of these challenges, assessing the safety of trees typically involves conducting a non-destructive winching test in the field. In this test, a windlass/jack is used to apply load through a cable onto the test tree, reacting against the root system of a nearby tree (Figure 1a; after Andreozzi et al. 2025). The moment applied to the test root system (M) is determined from the tension in the cable and the rotation of the base of the tree (and therefore of the root system) is measured by an inclinometer. Load is applied until the root system reaches a rotation (θ) of 0.25°. The moment-rotation data is then extrapolated to estimate the moment capacity (M_{ult}) by fitting the test data to the Wessolly and Erb model (Wessolly and Erb 1998):

$$\theta = \frac{1}{3}\tan\left(1.35\frac{M}{M_{ult}}\right) + \frac{1}{2}\left(\frac{M}{M_{ult}}\right)^2 - \frac{1}{10}\left(\frac{M}{M_{ult}}\right) \quad (1)$$

Using Equation 1, at θ = 0.25°, $M/M_{ult} \approx 0.4$, or alternatively, $M_{ult} \approx 2.5M(0.25°)$. This is shown in Figure 1b. The non-destructive test therefore uses a measure of stiffness to estimate ultimate capacity.

At the time of conducting a winching test, an established tree will have been loaded cyclically by ambient wind. It is well known from the literature on offshore foundations (e.g. Zhu et al. 2013) that cyclic loading can change the stiffness and capacity of a subsequent monotonic pushover. Additionally, the direction of pull in a winching test may be limited by the position of a nearby suitable tree for anchorage. Furthermore, anchorage to such a tree may not represent the predominant wind direction in which cyclic preconditioning has occurred. There has only recently been field study of cyclic loading and directionality effects on trees (Marrazzo et al. 2026) and this has been limited to a maximum of 10 cycles.

This paper presents the results of a preliminary study exploring the effect of cyclic loading on monotonic pushover capacity using 1-*g* physical model tests of 1:20 scale tree root systems. Up to 100 cycles of loading and different loading directions are considered, to explore potential implications for the use and interpretation of field winching tests.

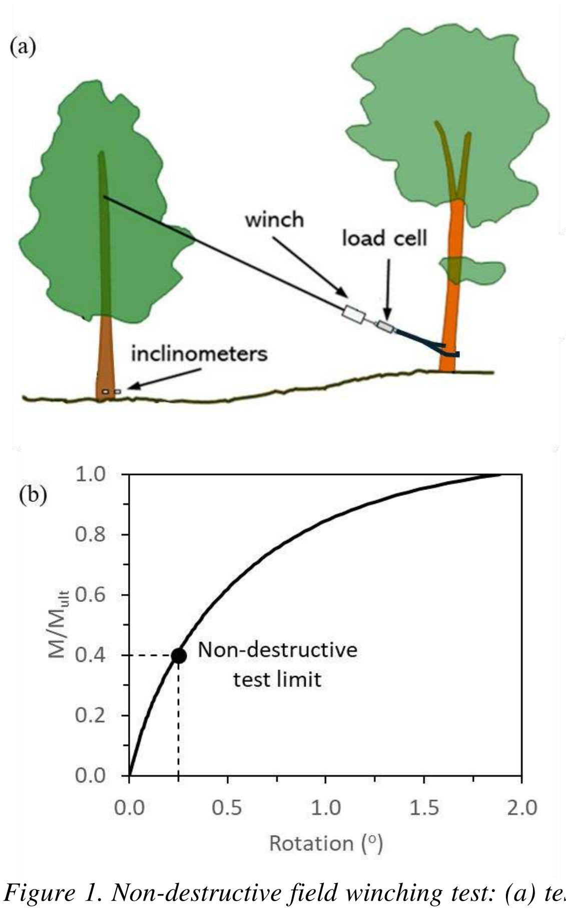

Figure 1. Non-destructive field winching test: (a) test set-up; (b) Interpretation using the Wessolly and Erb method (Equation 1)

2 REVIEW OF 1-G SCALING LAWS

Zhang et al. (2020) conducted both centrifuge and 1-*g* scale model tests of 3D-printed model root system analogues to determine suitable scaling laws for 1-*g* tests. These tests were conducted in dry and fully saturated coarse-grained soil (a 70% sand 30% non-plastic silt mix). These scaling laws are briefly reviewed here so that the 1-*g* model test results in this paper can be expressed at prototype scale. The developed scaling laws are shown in Table 1, where the first column (*N*-*g* (sat.)) presents the conventional scaling laws for tests conducted on 1:*N* scale models in saturated soil when tested on the centrifuge. The second column (1-*g* (sat.)) represents the conventional scaling laws for tests conducted on 1:*<u>N</u>* scale models tested at 1-*g* (e.g. Wood, 2004).

A benefit of conducting 1-g tests is the ability to conduct tests more rapidly. To speed-up model preparation, dry soil can be used to represent a fully saturated soil for loading conditions that are fully drained, provided that the difference in effective unit weight (dry vs. buoyant) is accounted for on the effective stresses in the soil. The effective stresses at homologous points in a dry model will be γ_d/γ' times larger (where γ_d is dry unit weight and γ' is buoyant unit weight) than in a fully saturated model at the same geometrical scaling factor (1:*N*). Scaling laws for this case (using a 1-*g* dry model to represent a fully saturated prototype) are shown in Table 1 (1-*g* (dry)).

The reduced stress level will also influence the strength of the soil. In a 1-g test, the reduced effective stress will result in less suppression of dilation and a higher effective friction angle. For root-soil interaction problems, Zhang et al. (2020) proposed correcting for this effect by multiplying by the ratio of passive earth pressure coefficient between model (K_{pm}) and prototype (K_{pp}). This is because capacity is proportional to the passive transverse resistance generated by pulling the roots through the soil (using a laterally loaded circular pile analogy). A similar approach has been proposed for 1-*g* testing of other systems that rely on generating passive resistance (e.g. seabed ploughs; Brown et al. 2015). Scaling laws for this case (assuming a dry 1-*g* model) are shown in the final column of Table 1 (1-*g* (dil. corr.)).

Figure 2 demonstrates application of the scaling laws in Table 1 to a 3D printed model tree root system, using data from Zhang et al. (2020). Values of K_p were determined using:

$$K_p = \frac{1+\sin\phi'}{1-\sin\phi'} \tag{2}$$

where friction angles were measured at appropriate stress levels using a model CPT probe. The data in Figure 2 clearly show an apparent overstrength if dilation is not accounted for (i.e. when using 1-g dry). The difference in dilation (and therefore K_{pm}/K_{pp}) was large for the soil tested, but correcting for this results in prototype results which closely match those obtained from the centrifuge at prototype scale. A similar good match was shown for a contrasting root system geometry in Zhang et al. (2020).

Table 1. 1-g scaling laws (model/prototype) for this study.

Quantity	***N*-*g* (sat.)**	**1-*g* (sat.)**	**1-*g* (dry)**	**1-*g* (dil. corr.)**
Length	$\frac{1}{N}$	$\frac{1}{N}$	$\frac{1}{N}$	$\frac{1}{N}$
Acceleration	N	1	1	1
Mass density	1	1	$\frac{\gamma_d}{\gamma'}$	$\frac{\gamma_d}{\gamma'}$
Force	$\frac{1}{N^2}$	$\frac{1}{N^3}$	$\frac{1}{N^3}\cdot\frac{\gamma_d}{\gamma'}$	$\frac{1}{N^3}\cdot\frac{\gamma_d}{\gamma'}\cdot\frac{K_{pm}}{K_{pp}}$
Moment	$\frac{1}{N^3}$	$\frac{1}{N^4}$	$\frac{1}{N^4}\cdot\frac{\gamma_d}{\gamma'}$	$\frac{1}{N^4}\cdot\frac{\gamma_d}{\gamma'}\cdot\frac{K_{pm}}{K_{pp}}$

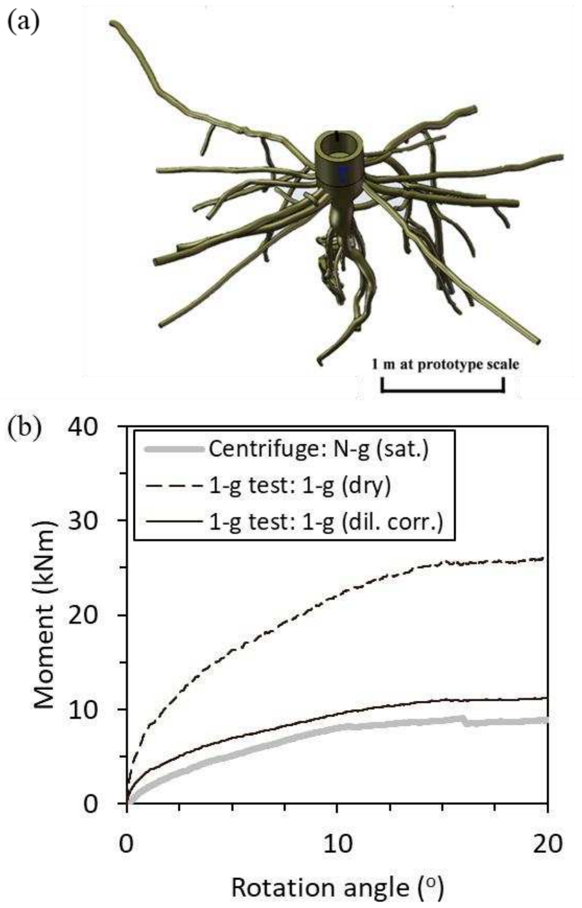

Figure 2. Validation of 1-g scaling laws: (a) 1:20 model root system tested; (b) prototype responses (data from Zhang et al., 2020).

3 METHODOLOGY

For the tests presented herein, a 1:20 scale model tree root system, similar to that shown in Figure 2, was 3D printed in Acrilonitrile Butadiene Styrene (ABS) plastic. The geometry was simplified to consist of horizontal, straight lateral roots and vertical, straight sinker roots only, to simplify any future numerical simulation of the tests (Figure 3a). A wooden (pine) model trunk was attached to a coupler on the top using an epoxy resin.

The root system was temporarily suspended above an aluminium alloy model container of internal size 800 × 500 mm, 500 mm deep (Figure 3b). This container had been prefilled with air pluviated HST95 silica sand to a density of 1.67 Mg/m^3 to fill the lower section of the box with a layer 180 mm thick. Above this, a 'test' layer of the same mix of 70% HST95 sand and 30% A50 silica silt used in Zhang et al. (2020) was air pluviated around the suspended model root system. This was conducted through a 1.18 mm sieve at a fixed

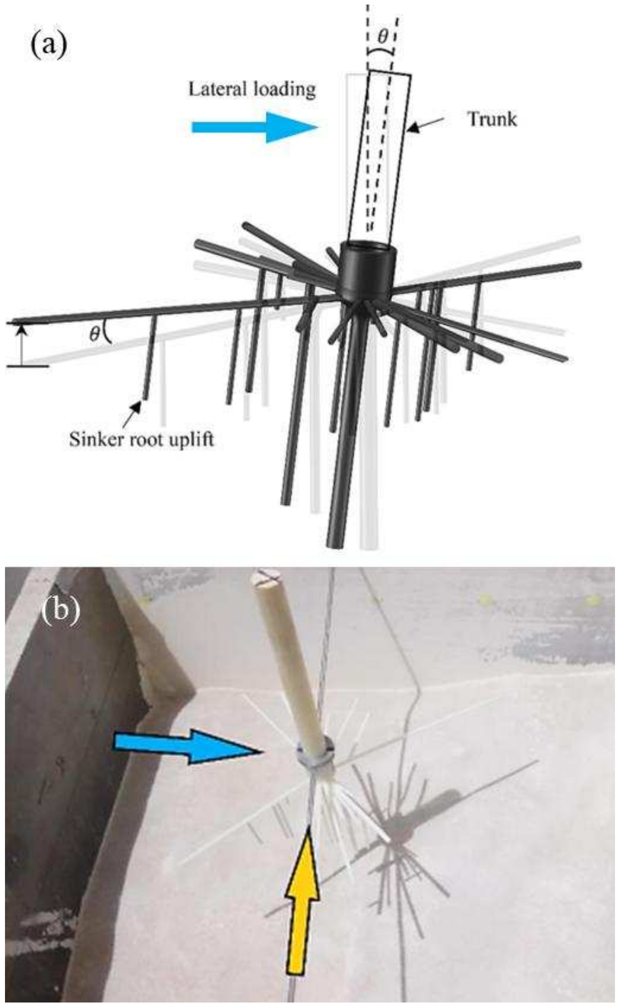

Figure 3. 1-g model testing: (a) root architecture; (b) model preparation, showing loading directions (blue = windward; orange = perpendicular)

height of 450 mm to achieve a relative density of ~50% to a thickness of 210 mm. The temporary root model supports shown in Figure 3b were carefully removed once the model root system was fully buried.

Lateral load testing was conducted using a GDSFA electromechanical force actuator (GDS instruments, UK) of stroke 100 mm. This had internal force and displacement measurement, recorded to a precision of ± 0.05N and ± 0.005 mm, respectively. All horizontal loading was applied at a point on the trunk 60 mm above the top of the root system, to generate moment. Loading was conducted in one of two directions, as shown in Figure 3b. The blue arrow represents loading in the windward direction (based on the site at which the root architecture in Figure 2a was originally measured, see Zhang et al. 2020 for further information). The orange arrow represents the direction perpendicular to this.

Two tests (tests 1 and 2) were initially conducted using a monotonic push to a rotation of 20° under displacement control at 1 mm/min. These tests represented drained soil response and were used to determine the pushover response of the root system in the windward and perpendicular directions under virgin loading. The two cases were tested to determine whether there is a strong load-directionality effect.

Subsequently, four further tests (tests 3 – 6) applied a packet of one-way cyclic loading under force control, followed by a post-cyclic monotonic push under displacement control. Each cycle (load + unload) was run over a period of 30 minutes to ensure a slow loading rate with no inertial effects (i.e. cyclic, rather than dynamic response). Across these tests, the target magnitude ($|M_{cyc}|$) and number of cycles (n) was varied, as was the direction of the cyclic loading relative to the subsequent push-over. A summary of the configuration of each test is provided in Table 2.

Table 2. Test programme summary.

ID	Pre-cycle push dir.	Cycle dir.	n	$\left\|\frac{M_{cyc}}{M_{ult}}\right\|$	Post-cycle push dir.
1	*W*	–	–	–	–
2	*P*	–	–	–	–
3	–	*W*	*100*	*0.43*†	*W*
4	–	*P*	*50*	*0.43*‡	*P*
5	–	*P*	*50*	*0.25*‡	*P*
6	–	*W*	*100*	*0.41*†	*P*

† M_{ult} *as determined in test 1 for windward (W) push.*
‡ M_{ult} *as determined in test 2 for perpendicular (P) push.*

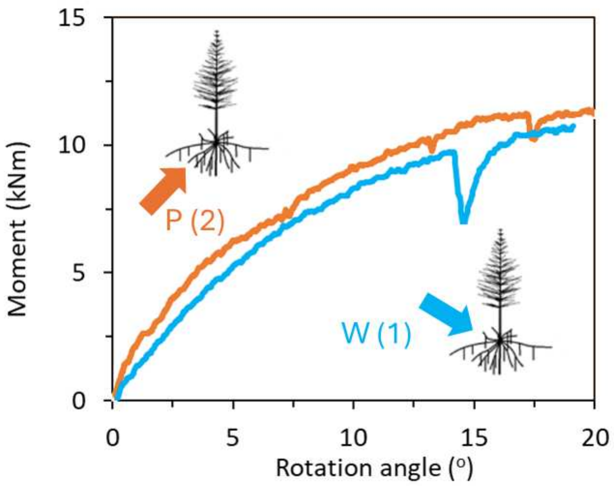

Figure 4. Pushover curves for monotonic loading on virgin soil (test numbers in parentheses).

4 RESULTS

4.1 Monotonic capacity (architecture effect)

Figure 4 shows the monotonic pushover curves for tests 1 and 2. The sudden drops in moment are associated with the breakage of discrete roots (verified by post-test excavation). It can be seen that there is a negligible difference in response between the two directions of push, indicating that the specific root system used did not have a strong bias in root location. Such bias can sometimes occur in field trees based on biological adaptation to a predominant direction of wind action.

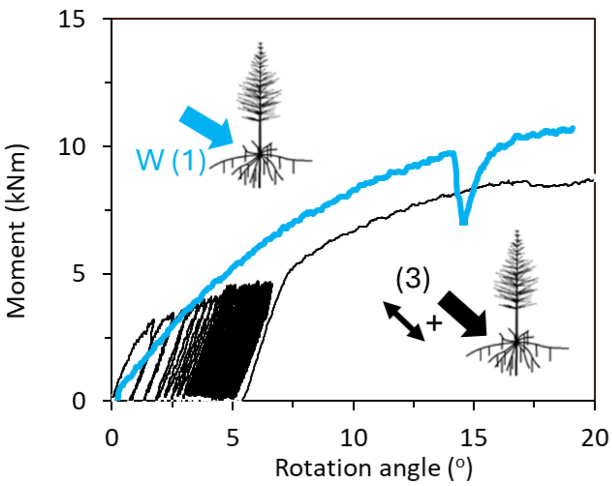

Figure 5. Effect of cyclic loading (preconditioning) on monotonic pushover curve – windward loading (test numbers in parentheses).

4.2 Effect of cyclic preconditioning on monotonic response

Figure 5 shows the effect of previous cyclic loading on monotonic response in the windward direction (i.e. from test 3, with test 1 as a monotonic comparator). In this direction of loading, the effect of the load cycles is to increase the stiffness of subsequent monotonic response, while reducing the capacity. Figure 6 shows similar responses for the root systems loaded in the perpendicular direction. These similarly show an increase in stiffness in the pushover response following cyclic loading, although the effect on post-cyclic capacity is less clear. In Figure 6a, the magnitude of the cyclic loading is of a similar magnitude to that shown in Figure 5, but the post cyclic capacity is increased. This appears to demonstrate that the physical position and orientation of the roots in the soil, relative to the direction of cyclic and monotonic loading, is important. This was not the case for monotonic pushover in virgin conditions (Figure 4). This may at least partially explain the significant scatter in empirical methods of capacity prediction where these are based on average/aggregated root system properties (e.g. total root volume or root plate geometry).

Figure 6b shows a reduction in capacity post-cycling. Comparing with Figure 6a, this suggests that the magnitude of the cyclic loading to which a tree has previously been subjected (e.g. due to high winds in previous strong storms) may affect the resulting pushover capacity. This demonstrates the potential importance of conducting non-destructive characterisation tests in the field, particularly if the rotational stiffness measured in such a test (i.e. at 0.25° or $0.4M_{\mathrm{ult}}$; Figure 1b) remains indicative of the ultimate moment capacity. This is discussed further in Section 5.

Figure 7 directly compares the post-cyclic re-zeroed and virgin monotonic responses for cases where the cyclic loading and subsequent pushover are in the same direction (windward cycling + windward pushover; test 3; Figure 7a) and when they are in different directions (windward cycling + perpendicular pushover; test 9; Figure 7b). The comparative virgin pushovers in each case had identical performance (Figure 4). As previously, there is consistency in the post-cyclic stiffness increasing in both cases due to cyclic preconditioning/shakedown. However, there is an apparent difference in effect on M_{ult}. The case having both cyclic and monotonic loads in the same direction (Figure 7a) demonstrates a reduction in capacity, while the case with the two loading stages in different directions (Figure 7b)

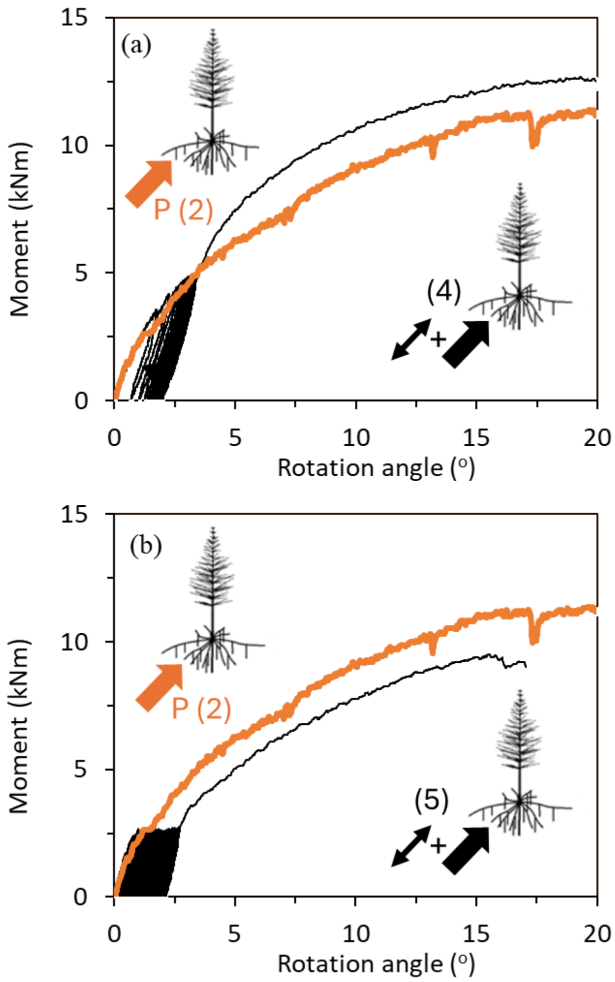

Figure 6. Effect of cyclic loading (preconditioning) on monotonic pushover – perpendicular loading (test numbers in parentheses): (a) $|M_{cyc}/M_{ult}|$ = 0.43; (b) $|M_{cyc}/M_{ult}|$ = 0.25

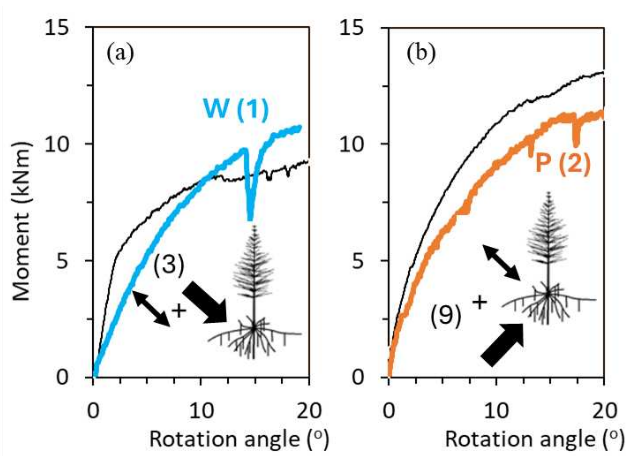

Figure 7. Effect of direction of cyclic loading on monotonic pushover (test numbers in parentheses): (a) windward cycling + windward pushover; (b) windward cycling + perpendicular pushover

exhibits an increase. This suggests that it is important to conduct non-destructive testing on trees in the direction which is most critical for hazard assessment (e.g. towards an overhead line), even if this means installing a temporary anchorage if no suitable nearby tree is available for anchorage. These patterns of change are the same as those observed in Figure 5 and Figure 6a (which had a similar magnitude of cyclic loading), so it may be that the effect of testing a tree in the field in a different direction to that in which it has been predominantly loaded by wind is not significant. Further testing is required to explore this further.

5 IMPLICATIONS FOR FIELD TEST INTERPRETATION

The commonly used Wessolly and Erb method (Equation 1) uses a measure of stiffness (from the non-destructive winching test) to estimate ultimate capacity, by assuming that any test data can be fitted to the proposed curve. From Equation 1, the ratio of rotational stiffness (K) to M_{ult} for a monotonic, non-destructive test is a fixed value:

$$K = \frac{M}{\theta} = \frac{0.4M_{ult}}{0.25^o} \quad (3)$$

Converting θ into radians, $K/M_{ult} \approx 92$. From Figure 8, the ratios of K/M_{ult} observed in the model tests are much lower than these. This questions the suitability of Equation 1 to reliably predict overturning capacities in different situations. It can further be seen that under virgin loading conditions (tests 1 – 2), defining the stiffness at $\theta = 0.25^o$ or $M = 0.4M_{ult}$ results in very different values of K/M_{ult}. This suggests that the Wessolly and Erb model does not represent such loading conditions well. However, with the application

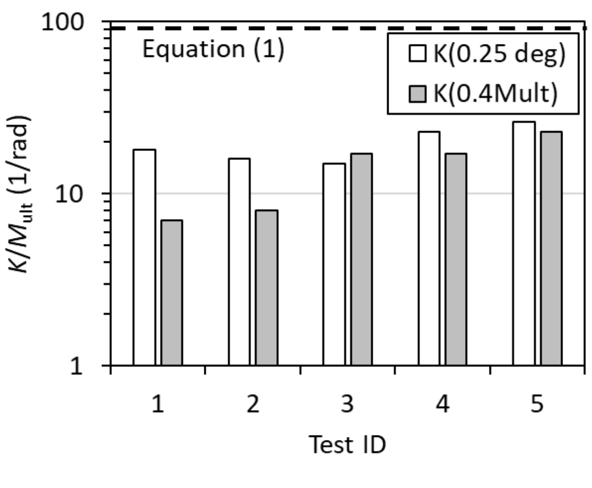

Figure 8. Ratio of stiffness (using non-destructive test protocol) to moment capacity.

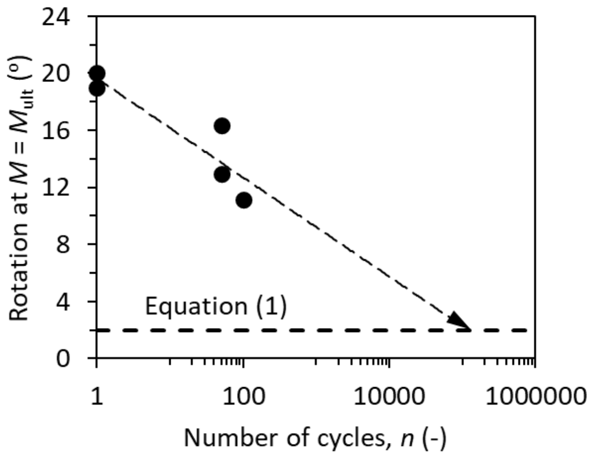

Figure 9. Rotation to peak as a function of previous cyclic loading.

of cyclic loading (tests 3 – 5) values of K/M_{ult} derived from the two definitions appear to converge and increase in magnitude. This suggests that shakedown under cyclic (wind) loading may justify the continued use of a single curve to fit non-destructive test data and extrapolate to predict capacity.

However, it is also clear from Figures 4 – 7 that none of the tests reached peak capacity at $\theta = 2^o$ as suggested by Equation 1 (and Figure 1b). Zhang et al. (2023) have previously demonstrated through centrifuge testing that the rotation at M_{ult} (under virgin loading conditions) is controlled by the depth of the groundwater table and the consequent degree of saturation of the soil surrounding the roots. Fully saturated conditions were found to give large rotations at peak (~20°, consistent with those for tests 1 and 2 in this study), with much smaller values being achieved for partially saturated cases (~5 °). Other authors have found similar ranges of rotation-to-peak from field testing. For example, testing of *Pinus pinaster* in a sandy soil by Défossez et al. (2021) resulted in a range of rotations-to-peak between 6 – 20°. For the model tests in this paper, it would appear that cyclic loading may also play a role in the value of θ at M_{ult}. Although there is limited data, Figure 9 tentatively suggests that shakedown under cyclic (wind) loading results in a reduction of rotation-to-peak in subsequent monotonic pushover. This, again, suggests continued potential justification for defining a unique rotation at which to define stiffness if the tree has undergone tens of thousands or hundreds of thousands of cycles of prior loading below the ultimate limit stat. However, any rotation so defined would also need to be a function of the groundwater conditions at the time of testing.

6 CONCLUSIONS

This paper has presented some preliminary 1-g model tests exploring the influence of (one-way) cyclic loading on the monotonic pushover response of a model tree root system, as might be measured in non-destructive field winching tests. 1-*g* scaling laws (validated against centrifuge test data) were presented so that 1-*g* model test results can be presented at prototype scale. Measured monotonic responses did not support the use of the popular Wessolly and Erb interpretative model in virgin soil conditions. However, the tests provided evidence that preconditioning/shakedown of the tree and root system under cyclic loading below the ultimate limit state (e.g. from ambient wind throughout its life) may result in convergence towards a single non-dimensional pushover curve shape. However, further data considering different root architectures and larger numbers of cycles would be required to confirm this.

ACKNOWLEDGEMENTS

The third author would like to acknowledge the financial support of the China Scholarship Council (CSC) and the Norman Fraser Design Trust. Gary Callon (University of Dundee) is also acknowledged for his assistance in printing the root models used in this study.

REFERENCES

Achim, A. and Nicoll, B. C. (2009). Modelling the anchorage of shallow-rooted trees. *Forestry,* 82(3): 273–284. https://doi.org/10.1093/forestry/cpp004

Andreozzi, M., Marrazzo, G., Marsiglia, A., Boldrin, D., Castellanza, R. P., Knappett, J. A. and Ciantia, M. O. (2025) On the Uprooting Stability of Trees: Combined Loading Effect on Tree Stability Assessment. *Forests*,16: 1780. https://doi.org/10.3390/f16121780

Brown, M. J., Bransby, M. F., Knappett, J. A., Tovey, S., Lauder, K. and Pyrah, I. (2015) The effect of buried fibres on offshore pipeline plough performance. *Ocean Engineering*, 108: 760-768. https://doi.org/10.1016/j.oceaneng.2015.08.022

Dattola, G., Ciantia, M. O., Galli, A., Blyth, L., Zhang, X., Knappett, J. A., Castellanza, R., Sala, C. & Leung, A. K. (2020). A macroelement approach for the stability assessment of trees. In: *Geotechnical research for land protection and development: proceedings of CNRIG 2019* (eds F. Calvetti, F. Cotecchia, A. Galli and C. Jommi), pp. 417–426, Cham, Switzerland: Springer https://doi.org/10.1007/978-3-030-21359-6_44

Défossez, P., Veylon, G., Yang, M., Bonnefond, J. M., Garrigou, D., Trichet, P. & Danjon, F. (2021) Impact of soil water content on the overturning resistance of young Pinus pinaster in sandy soil. *Forest Ecology and Management,* 480: 118614. https://doi.org/10.1016/j.foreco.2020.118614

Jakob, M. and Lambert, S. (2009). Climate change effects on landslides along the southwest coast of British Columbia. *Geomorphology,* 107(3–4): 275–284, https://doi.org/10.1016/j.geomorph.2008.12.009

Marrazzo, G., Andreozzi, M., Boldrin, D., Galli, A., and Ciantia, M. O. (2026) Real-scale tests on the cyclic response of trees under toppling loads: experimental investigation and geotechnical interpretative framework. *Canadian Geotechnical Journal (online ahead-of-print)*. https://doi.org/10.1139/cgj-2025-0314

McCarthy, J. K., Hood, I. A., Brockerhoff, E. G., Carlson, C. A., Pawson, S. M., Forward, M., Walbert, K. and Gardner, J. F. (2010) Predicting sapstain and degrade in fallen trees following storm damage in a Pinus radiata forest. *Forest Ecology and Management,* 260(9):1456–1466. https://doi.org/10.1016/j.foreco.2010.07.044

Schmidlin, T. W. (2009). Human fatalities from wind-related tree failures in the United States, 1995–2007. *Natural Hazards*, 50(1): 13–25. https://doi.org/10.1007/s11069-008-9314-7

Wessolly, L. and Erb, M. (1998) *Handbuch der Baumstatik und Baumkontrolle* (in German). Patzer-Verlag, Berlin.

Wood DM (2004) *Geotechnical modelling*. Spon Press, Abingdon.

Zhang, X., Knappett, J. A., Leung, A. K., Ciantia, M. O., Liang, T. and Danjon, F. (2020) Small-scale modelling of root–soil interaction of trees under lateral loads. *Plant and Soil,* 456(1–2): 289–305. https://doi.org/10.1007/s11104-020-04636-8

Zhang, X., Knappett, J. A., Leung, A. K., Ciantia, M. O., Liang, T. and Nicoll, B. C. (2023) Centrifuge modelling of root–soil interaction of laterally loaded trees under different loading conditions. *Géotechnique* 73(9): 766–780. https://doi.org/10.1680/jgeot.21.00088

Zhu, B., Byrne, B. W. and Houlsby, G. T. (2013) Long-Term Lateral Cyclic Response of Suction Caisson Foundations in Sand. *Journal of Geotechnical and Geoenvironmental Engineering*, 139(1): 73-83. https://doi.org/10.1061/(ASCE)GT.1943-5606.0000738